**Applied Mathematics E-Notes, 19(2019), 456-464** © ISSN 1607-2510
Available free at mirror sites of http://www.math.nthu.edu.tw/∼amen/

# An Application Of Khuri's Biorthogonality Condition On Stokes Flow In A Rectangular Cavity*

Halis Bilgil†

Received 3 July 2018

**Abstract**

The paper present a different semi-analytical solutions for the Stokes flow in a rectangular cavity by using the biorthogonality condition of the eigenfunctions. Firstly, the biorthogonality condition for rectangular cavity is applied on Stokes Flow problem. Secondly, the biorthogonality condition and the new solution is verified against results available in the literature. Further, it has been found that this solution mechanism is efficient and it can be successfully used to obtain flow structures and bifurcations.

## 1 Introduction

Flow inside a rectangular cavity has been studied extensively far more than two decades and is one of the most popular fluid problems in the fluid mechanics. In the available literature, it is possible to find numerous studies on lid-driven cavity flow [1, 2, 7, 8, 11, 15]. Joseph and Sturges [12] were the first to formulate and solve the Stokes flow problem analytically by expressing the streamfunction, $\psi$, as an infinite series of eigenfunctions and determining the associated series coefficients using Smith's biorthogonality condition [19]. Subsequently, Shankar [17] applied a least-squares method rather than a biorthogonality condition to determine the coefficients in the infinite series for the same problem. Gaskell et al. [4] compared the accuracy of the above least-squares and biorthogonal approaches by examining the convergence of the streamfunction and the horizontal velocity component to the upper boundary conditions. Their results for the $\psi = 0$ condition are better via the biorthogonal method than via the least-squares method, but for the velocity conditions the situation is reversed. They also compared values of the streamfunction in the cavity interior and found that the streamfunction values are extremely close and almost unaffected by the choice of either the Shankar [17] or the Joseph and Sturges [12] coefficient determination methods.

A new eigenfunction expansion method for solving Stokes flow problems in cavities that arise in fluid dynamics has been developed by Khuri [13]. The method leads to the development of a set of eigenfunctions, adjoint eigenfunctions, biorthogonality conditions, and an algorithm for the computation of the coefficients of the eigenfunction

*Mathematics Subject Classifications: 00A05, 35Q35, 76D99, 82B23, 65N99.
†Department of Mathematics, Aksaray University, Aksaray 68100, Turkey

expansion. Subsequently, Khuri [14] introduced a biorthogonality condition for rectangular regions. This biorhogonality conditions aims to solve the Stokes flow problem more easily and apparent than above analytical solution methods.

This article has two aims: first, to find a new analytical solution of Stokes flow problem in a rectangular cavity by using Khuri's biorthogonality conditions; secondly, to verify the accuracy and efficiency of Khuri's theorem to solve Stokes flow problems in comparison to the previous solutions.

## 2 Biorthogonality Conditions

The fourth-order boundary value problem and the boundary conditions are given by,

$$(P_0(r)y''(r))'' + (P_1(r;\alpha)y'(r))' + P_2(r;\alpha)y(r) = 0, \quad r \in [r_1, r_2], \tag{1}$$

$$y(r_1) = y(r_2) = y'(r_1) = y'(r_2) = 0. \tag{2}$$

The biorthogonality condition for the boundary value problem given in following Khuri's Theorem [1].

THEOREM 1. Consider the boundary value problem given in Eq.(1) and (2) where $P_0(r)$, $P_1''(r;\alpha)$, $P_2(r;\alpha)$ are continuous and $P_0(r) \neq 0$ on $r_1 \leq r \leq r_2$. $P_i$ in Eq.(1) is a polynomial of degree at most $i$ in the parameter $\alpha$, in particular, let $P_1(r;\alpha) = p_{11}(r)\alpha + p_{12}(r)$, and we require

$$P_1^2(r;\alpha) - 4P_0(r)P_2(r;\alpha) = p_{31}(r)\alpha + p_{32}(r),$$

$$p_{11}^2(r) + p_{31}^2(r) \not\equiv 0.$$

Then with $P_n^*$ defined by

$$P_n^* = \int_{r_1}^{r_2} \left[\phi_2^{(n)}(r),\ \phi_1^{(n)}(r)\right] B(r) \begin{bmatrix} \phi_1^{(n)}(r) \\ \phi_2^{(n)}(r) \end{bmatrix} dr,$$

we have the following biorthogonality condition:

$$\int_{r_1}^{r_2} \left[\phi_2^{(m)}(r),\ \phi_1^{(m)}(r)\right] B(r) \begin{bmatrix} \phi_1^{(n)}(r) \\ \phi_2^{(n)}(r) \end{bmatrix} dr = P_n^*\delta_{mn},$$

where $\delta_{mn}$ is the Kronecker's delta,

$$B(r) = \begin{pmatrix} -\frac{p_{11}(r)}{2P_0(r)} & 0 \\ \frac{1}{2}p_{11}''(r) + \frac{1}{4}\frac{p_{31}(r)}{2P_0(r)} & -\frac{p_{11}(r)}{2P_0(r)} \end{pmatrix}$$

with

$$\phi_1^{(n)}(r) = y_n(r),$$

$$\phi_2^{(n)}(r) = P_0(r)y_n''(r) + \frac{1}{2}P_1(r;\alpha_n)y_n(r).$$

Here $y_i$ is an eigenfunction of Eq.(1) corresponding to the eigenvalue $\alpha_i$.

# 3 The Boundary Value Problem For Rectangular Cavity and Biorthogonality Condition

## 3.1 The Formulation of Flow Problem

A two-dimensional rectangular cavity $\nu = \{x, y : -1 \leq x \leq 1, -A \leq y \leq A\}$ is filled with incompressible fluid (Fig. 1). The boundaries $x = \pm 1$ are fixed walls, $y = A$ and $y = -A$ are two moving lids which translate with speeds $U_1$ and $U_2$ in the horizontal direction respectively, thus setting the fluid into motion.

Under Stokes's approximation for the creeping flow the streamfunction $\psi(x, y)$ satisfies the two-dimensional biharmonic equation

$$\nabla^4 \psi(x, y) = \left( \frac{\partial^2}{\partial x^2} + \frac{\partial^2}{\partial y^2} \right)^2 \psi(x, y) = 0. \tag{3}$$

The streamfunction is set equal to zero on the boundaries of the cavity, and the no-slip conditions for the upper and lower lids and side walls are

$$\psi(\pm 1, y) = 0, \quad \frac{\partial \psi}{\partial x}(\pm 1, y) = 0, \tag{4}$$

$$\psi(x, \pm A) = 0, \tag{5}$$

$$\frac{\partial \psi}{\partial y}(x, A) = U_1, \quad \frac{\partial \psi}{\partial y}(x, -A) = U_2. \tag{6}$$

The boundary-value problem has a separation of variables solution for $\psi$ of the form,

$$\psi(x, y) = \sum_{-\infty}^{\infty} \left[ A_n e^{\lambda_n (y - A)} + B_n e^{-\lambda_n (y + A)} \right] \frac{\phi_1^{(n)}(x, \lambda_n)}{\lambda_n^2} \tag{7}$$

where $A_n$ and $B_n$ are complex coefficients, the $\lambda_n$ are complex eigenvalues and $\phi_1^{(n)}(x, \lambda_n)$ are even Papkovich-Fadle eigenfunctions [2-4]. The eigenfunctions are given by

$$\phi_1^{(n)}(x, \lambda_n) = \lambda_n \sin(\lambda_n) \cos(\lambda_n x) - \lambda_n x \sin(\lambda_n x) \cos(\lambda_n). \tag{8}$$

The parameters $\lambda_n$ are complex eigenvalues determined by the side wall conditions Eq.(4), which yield the eigenvalue equation, $\sin 2\lambda_n = -2\lambda_n$. The $\lambda_n$ eigenvalues may be determined by the simple Newton iteration procedure described by Robbins and Smith [5]. Table of the eigenvalues can be seen in [10]. The flow is governed by two physical control parameters: the cavity aspect ratio $A$ and the ratio ($S = \frac{U_2}{U_1}$) of the lower to the upper lid speed.

## 3.2 The Biorthogonality Condition For Rectangular Cavities and Solution

The following biorthogonality condition for rectangular cavities is given by Khuri [7],

$$\int_{-1}^{1} \left[ \phi_2^{(m)}(x),\ \phi_1^{(m)}(x) \right] B(x) \begin{bmatrix} \phi_1^{(n)}(x) \\ \phi_2^{(n)}(x) \end{bmatrix} dx = P_n^* \delta_{mn} \tag{9}$$

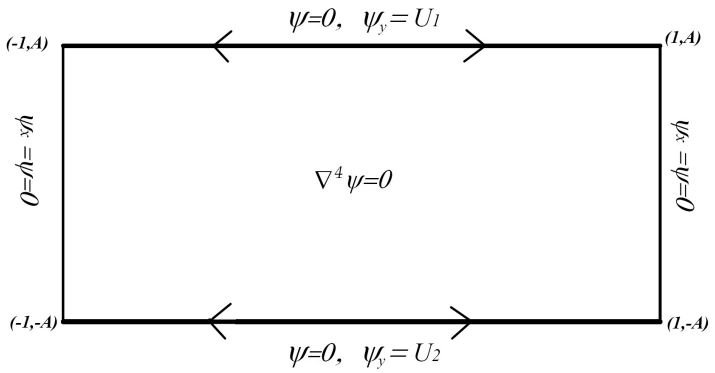


Fig. 1: The boundary value problem for the lid-driven cavity.

where

$$B(x) = \begin{pmatrix} -1 & 0 \\ 0 & -1 \end{pmatrix}$$

and

$$\phi_2^{(n)}(x,\lambda_n) = \left(\phi_1^{(n)}(x)\right)'' + \lambda_n^2 \phi_1^{(n)}(x) = -2\lambda_n^2 \cos(\lambda_n)\cos(\lambda_n x). \tag{10}$$

Eq.(7) must satisfy the boundary conditions Eq.(5) and (6); that is,

$$U_1 = \sum_{-\infty}^{\infty} \left[A_n - B_n e^{-2\lambda_n A}\right] \frac{\phi_1^{(n)}(x)}{\lambda_n}, \tag{11}$$

$$0 = \sum_{-\infty}^{\infty} \left[A_n + B_n e^{-2\lambda_n A}\right] \frac{\phi_1^{(n)}(x)}{\lambda_n^2}, \tag{12}$$

$$U_2 = \sum_{-\infty}^{\infty} \left[A_n e^{-2\lambda_n A} - B_n\right] \frac{\phi_1^{(n)}(x)}{\lambda_n}, \tag{13}$$

$$0 = \sum_{-\infty}^{\infty} \left[A_n e^{-2\lambda_n A} + B_n\right] \frac{\phi_1^{(n)}(x)}{\lambda_n^2}, \tag{14}$$

where $U_1$ and $U_2$ represent the velocities of the top and bottom lids. The other boundary conditions are used to find the $\lambda_n$ eigenvalues. The solution procedure up to here is almost the same with previous studies [6, 7, 8].

The critical step in determining $A_n$ and $B_n$ is to apply the biorthogonality condition Eq.(9) to equations (11)–(14). To prefare for this application of the biorthogonality condition, equations (11)–(12) are combined to give

$$\sum_{-\infty}^{\infty} \frac{1}{\lambda_n^2} \left(A_n + B_n e^{-2\lambda_n A}\right) \begin{pmatrix} \phi_1^{(n)}(x) \\ \phi_2^{(n)}(x) \end{pmatrix} - \sum_{-\infty}^{\infty} \frac{1}{\lambda_n^2} \left(A_n + B_n e^{-2\lambda_n A}\right) \begin{pmatrix} 0 \\ \phi_2^{(n)}(x) \end{pmatrix}$$

$$+\sum_{-\infty}^{\infty}\frac{1}{\lambda_n}\left(A_n-B_ne^{-2\lambda_nA}\right)\begin{pmatrix}0\\ \phi_1^{(n)}(x)\end{pmatrix}=\begin{pmatrix}0\\ U_1\end{pmatrix}. \tag{15}$$

Similarly, by coupling equations (13)–(14), rearranging terms, we get

$$\sum_{-\infty}^{\infty}\frac{1}{\lambda_n^2}\left(A_ne^{-2\lambda_nA}+B_n\right)\begin{pmatrix}\phi_1^{(n)}(x)\\ \phi_2^{(n)}(x)\end{pmatrix}-\sum_{-\infty}^{\infty}\frac{1}{\lambda_n^2}\left(A_ne^{-2\lambda_nA}+B_n\right)\begin{pmatrix}0\\ \phi_2^{(n)}(x)\end{pmatrix}$$
$$+\sum_{-\infty}^{\infty}\frac{1}{\lambda_n}\left(A_ne^{-2\lambda_nA}-B_n\right)\begin{pmatrix}0\\ \phi_1^{(n)}(x)\end{pmatrix}=\begin{pmatrix}0\\ U_2\end{pmatrix}. \tag{16}$$

The operator

$$\int_{-1}^{1}\left[\phi_2^{(m)}(x),\ \phi_1^{(m)}(x)\right]\begin{pmatrix}-1&0\\ 0&-1\end{pmatrix}\begin{bmatrix}\cdot\\ \cdot\end{bmatrix}dx=P_n^*\delta_{mn}$$

is then applied to Eq.(15) and (16) to yield

$$\sum_{-\infty}^{\infty}\frac{1}{\lambda_n^2}\left(A_n+B_ne^{-2\lambda_nA}\right)P_m-\sum_{-\infty}^{\infty}\frac{1}{\lambda_n^2}\left(A_n+B_ne^{-2\lambda_nA}\right)V_m$$
$$+\sum_{-\infty}^{\infty}\frac{1}{\lambda_n^2}\left(A_n-B_ne^{-2\lambda_nA}\right)=G_m,$$

$$\sum_{-\infty}^{\infty}\frac{1}{\lambda_n^2}\left(A_ne^{-2\lambda_nA}+B_n\right)P_m-\sum_{-\infty}^{\infty}\frac{1}{\lambda_n^2}\left(A_ne^{-2\lambda_nA}+B_n\right)V_m$$
$$+\sum_{-\infty}^{\infty}\frac{1}{\lambda_n^2}\left(A_ne^{-2\lambda_nA}-B_n\right)=g_m,$$

where

$$G_m=\int_{-1}^{1}\left[\phi_2^{(m)}(x),\ \phi_1^{(m)}(x)\right]\begin{pmatrix}-1&0\\ 0&-1\end{pmatrix}\begin{bmatrix}0\\ U_1\end{bmatrix}dx=-4U_1,$$
$$g_m=\int_{-1}^{1}\left[\phi_2^{(m)}(x),\ \phi_1^{(m)}(x)\right]\begin{pmatrix}-1&0\\ 0&-1\end{pmatrix}\begin{bmatrix}0\\ U_2\end{bmatrix}dx=-4U_2,$$
$$P_m=\int_{-1}^{1}\left[\phi_2^{(m)}(x),\ \phi_1^{(m)}(x)\right]\begin{pmatrix}-1&0\\ 0&-1\end{pmatrix}\begin{bmatrix}\phi_1^{(n)}(x)\\ \phi_2^{(n)}(x)\end{bmatrix}dx,$$
$$V_{mn}=\int_{-1}^{1}\left[\phi_2^{(m)}(x),\ \phi_1^{(m)}(x)\right]\begin{pmatrix}-1&0\\ 0&-1\end{pmatrix}\begin{bmatrix}0\\ \phi_2^{(n)}(x)\end{bmatrix}dx,$$

and

$$W_{mn}=\int_{-1}^{1}\left[\phi_2^{(m)}(x),\ \phi_1^{(m)}(x)\right]\begin{pmatrix}-1&0\\ 0&-1\end{pmatrix}\begin{bmatrix}0\\ \phi_1^{(n)}(x)\end{bmatrix}dx.$$

Equations (15) and (16) form an infinite set to be solved for the coefficients $A_n$, $B_n$ for $n=\pm1,\pm2,....$ They are determined as Eq.(15) and (16) are truncated after $N$ terms. In this case Eq.(15) and (16) yield $4N$ equations for the $4N$ unknowns.

# 4 Results

Figure 2 shows examples of streamline plots for $S = -1$ at which the lids move in opposite directions with equal speed ratio. It is seen that, the flow structure is symmetrical about $x$ and $y$-axis for all values of $A$. A single eddy occupies the cavity for $A = 0.36$ and $A = 0.7$, see Fig. 2a and 2b respectively. The single eddy has a center stagnation point in the cavity center. As the aspect ratio is increased from 0.7 there are four main stages in the development of the second and third eddies. In the first stage, a bifurcation appears at a critical value of $A$ and two additional stagnation points are generated in the cavity, (see Fig. 2c where $A = 1$).

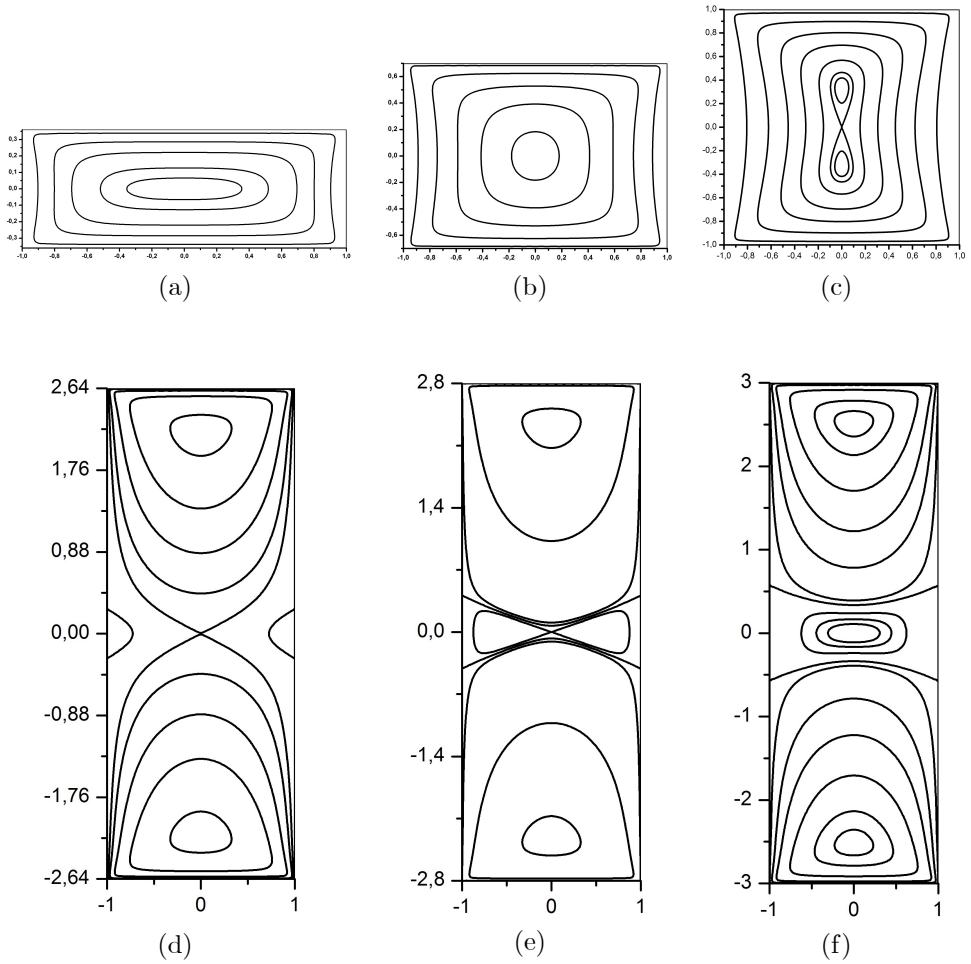


Fig. 2: Streamline for a double lid-driven cavity for $S = -1$. (a) $A = 0.36$ (b) $A = 0.7$ (c) $A = 1$ (d) $A = 2.64$ (e) $A = 2.8$ (f) $A = 3$.

As $A$ is increased further, two degenerate critical points appear on the two stationary side walls. In the third stage, the heteroclinic connections coalesce with each other at the interior saddle point to produce four heteroclinic connections between the saddle point and the four separation points on the side walls, as shown in Fig. 2d. As the aspect ratio is increased further, it is seen that there are two complete eddies within the cavity and between them a third is about to be created. Indeed, as $A$ is increased more the heteroclinic connections from the four separation points separate from the saddle point on the cavity center. There are now two heteroclinic connections crossing the cavity, each connected to separation points on the side walls, and between these two streamlines lies the saddle point on $(x, y) = (0, 0)$ with its separatrix enclosing two sub-eddies. As $A$ increases, the sub-eddy center lying left of the saddle on $y = 0$ approach the saddle point on $(x, y) = (0, 0)$ and coalesce, disappearing at a critical value of $A$ (Fig. 2e). This is a cusp (saddle-node) bifurcation. At this critical aspect ratio the formation of a third eddy, between the other two, is complete so that three eddies now occupy the cavity (Fig. 2f). This is a mechanism for eddy generation in which one eddy becomes three.

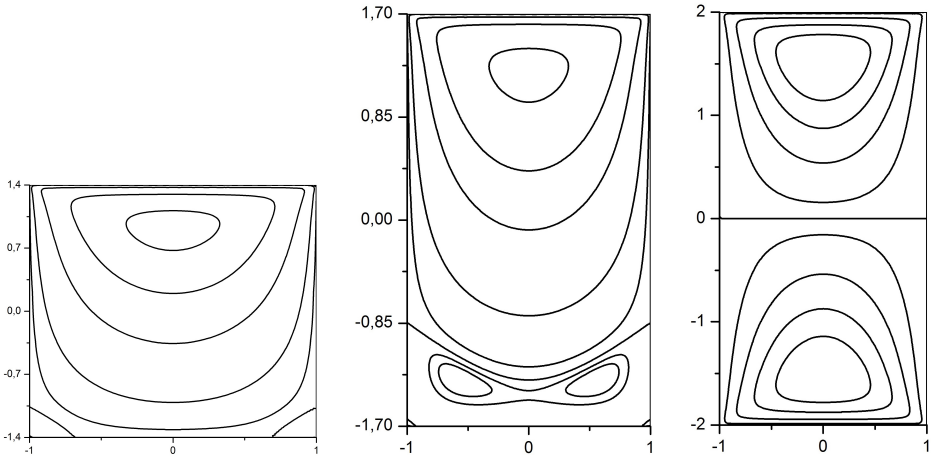


Fig. 3: Typical flow structures. (a) $S = 0,\ A = 1.4$ (b) $S = 0,\ A = 1.7$ (c) $S = 1,\ A = 2$.

Figure 3 shows the some flow structures for $S = 0$ (where $U_2 = 0$) and $S = 1$ at which the lids move in opposite directions with equal speed ratio respectively. These eddy genesis mechanisms are not new. They have been found before by several authors [6, 8, 9, 17, 10]. For this reason, the more detailed representation of the flow structures is not necessary.

| | $\lvert\psi(x,A)\rvert_{ave}$ | $\left\lvert\frac{\partial\psi}{\partial y}(x,A)-2\right\rvert_{ave}$ | $\lvert\psi(x,-A)\rvert_{ave}$ | $\left\lvert\frac{\partial\psi}{\partial y}(x,-A)-1\right\rvert_{ave}$ |
|---|---|---|---|---|
| *Present* | | | | |
| $N=20$ | $1.4052x10^{-3}$ | 0.1782 | $1.4614x10^{-4}$ | $5.0867x10^{-2}$ |
| $N=50$ | $3.5903x10^{-4}$ | $9.7694x10^{-2}$ | $2.7424x10^{-5}$ | $2.2853x10^{-2}$ |
| $N=100$ | $1.2531x10^{-4}$ | $6.3657x10^{-2}$ | $6.0344x10^{-6}$ | $1.1745x10^{-2}$ |
| *Joseps and Sturges* | | | | |
| $N=20$ | $2.1105x10^{-4}$ | 0.2021 | $2.7836x10^{-5}$ | $6.4283x10^{-2}$ |
| $N=50$ | $2.9736x10^{-4}$ | 0.6136 | $5.8074x10^{-6}$ | $2.6267x10^{-2}$ |
| $N=100$ | $2.0746x10^{-5}$ | 0.1297 | $1.1533x10^{-6}$ | $1.4809x10^{-2}$ |
| *Shankar* | | | | |
| $N=20$ | $1.0593x10^{-3}$ | 0.1266 | $5.2965x10^{-4}$ | $6.3301x10^{-2}$ |
| $N=50$ | $2.4924x10^{-4}$ | $6.2803x10^{-2}$ | $1.2462x10^{-4}$ | $3.1401x10^{-2}$ |
| $N=100$ | $7.5580x10^{-5}$ | $3.5213x10^{-2}$ | $3.7790x10^{-5}$ | $1.7606x10^{-2}$ |

Table 1: Satisfaction of horizontal wall boundary conditions for $U_1=2$, $U_2=1$, $A=5$.

Table 1 shows values of the streamfunction from the present study compared with those of Shankar and Joseph-Sturges on the cavity boundary. Here, averages are shown over 1000 equally spaced points in $x\in[0,1)$. All the tabulated results relate to a typical case in which $U_1=2$, $U_2=1$ and $A=5$. Remarkably good aggreement is seen between the present computations and those of Shankar and Joseph-Sturges [17, 12, 6].

# References

[1] H. Bilgil and F. Gürcan, Effect of the Reynolds number on flow bifurcations and eddy genesis in a lid-driven sectorial cavity, Jpn. J. Ind. Appl. Math., 33(2016), 343–360.

[2] A. Deliceoğlu and S. H. Aydın, Topological flow structures in an L-shaped cavity with horizontal motion of the upper lid, J. Comput. Appl. Math., 259(2014), part B, 937–943.

[3] P. H. Gaskell, M. D. Savage, J. L. Summers and H. M. Thompson, Modeling and analysis of meniscus roll coating, J. Fluid Mech., 298(1995), 113–137.

[4] P. H. Gaskell, M. D. Savage., J. L. Summers and H. M. Thompson, Creeping flow analyses of free surface cavity flows, J. Theor. Comput. Fluid Dynamics, 8(1996), 415–433.

[5] P. H. Gaskell, Gürcan, F., M. D. Savage. and H. M. Thompson, Stokes flow in a double-lid-driven cavity with free surface side-walls, Proc. Instn. Mech. Engrs, Part C: J. Mechanical Engineering Science, 212(1998), 387–403.

[6] P. H. Gaskell, M. D. Savage, J. L. Summers and H. M. Thompso, Stokes flow in closed, rectangular domains, Appl. Math. Model., 22(1998), 727–743,

[7] F. Gürcan, Streamline topologies in Stokes flow within lid-driven cavities, Theor. Comput. Fluid Dyn., 17(2003), 19–30.

[8] F. Gürcan, P. H. Gaskell, M. D. Savage and M. Wilson, Eddy genesis and transformation of Stokes flow in a double-lid-driven cavity, Proc. of The Instn. Mech. Eng. Part-C: J. Mec. Eng. Sci, 217(2003), 353–364.

[9] F. Gürcan, M. Wilson and M. D. Savage, Eddy genesis and transformation of Stokes flow in a double-lid-driven cavity. Part 2: deep cavities, Proc. of The Instn. Mech. Eng. Part-C: J. Mec. Eng. Sci, 220(2006), 1765–1774.

[10] F. Gürcan and H. Bilgil, Bifurcations and eddy genesis of Stokes flow within a sectorial cavity, European Journal of Mechanics-B/Fluids, 39(2013), 42–51

[11] C. J. Heaton, On the appearance of Moffatt eddies in viscous cavity flow as the aspect ratio varies, Physics of Fluid, 20(2008), 103102.

[12] D. D. Joseph and L. Sturges, The convergence of biorthogonal series for biharmonic and stokes flow edge problems: Part II, Siam., J. Appl. Math., 34(1978), 7–27.

[13] S. A. Khuri, Biorthogonal series solution of stokes flow problems in sectorial regions, Siam., J. Appl. Math., 56(1996), 19–39.

[14] S. A. Khuri, Biorthogonality condition for stokes flow in rectangular regions, Int. J. Comput. Math., 70(1999), 411–415.

[15] V. V. Meleshko, Steady Stokes flow in a rectangular cavity, Proc. R. Soc. London Ser. A, 452, (1996), 1999–2022.

[16] M. Scholle, A. Haas, N. Aksel, M. C. T. Wilson, H. M. Thompson and P. H. Gaskell, Competing geometric and inertial effects on local flow structure in thick gravity-driven fluid films, Physics of Fluids, 20(2008), 123101.

[17] P. N. Shankar, Three-dimensional eddy structure in a cylindrical container, J. Fluid Mechanics, 342(1997), 97–118.

[18] P. N. Shankar and M. D. Despande, Fluid mechanics in the driven cavity, Ann. Rev. Fluid Mech., 136(2000), 93–136..

[19] R. C. T. Smith, The bending of a semi-infinite strip, Australian J. Sci. Res. Ser. A, 5(1952), 227–237.